< x < d, - h_1 < z < η; R_3: - d < x < d, -h_3 < z < - h_2; R_4: - d < x < d, - h < z < - h_4 and R_5: - L < x < - d, - h < z < η, where η is the free surface elevation from mean water level.

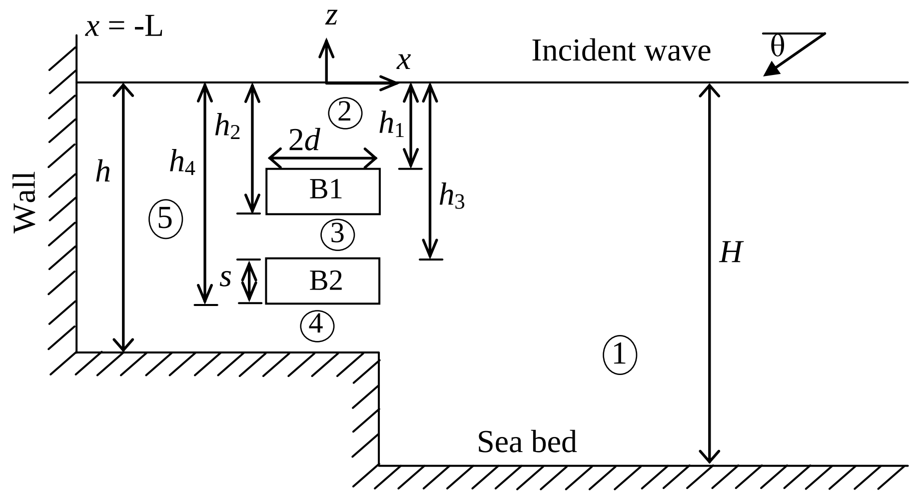

Fig.1 Schematic view of submerged prisms in semi-infinite fluid domain

Fluid of density ρ is considered inviscid, incompressible. The fluid motion is irrotational and simple harmonic in time, having angular frequency ω. Considering small-amplitude water wave theory, oblique water wave is adopted. The angle of interaction between the incident wave and structure is θ. Thus, the velocity potential $\Phi(x,y,z,t)$ can be written as $\Phi(x,y,z,t)=\mathrm{Re}[\phi(x,z)e^{i(k_y y-\omega t)}]$, where Re represents the real part and $k_y = k_0 \sin\theta$ being the y-component of the wavenumber k_0. Therefore, the spatial velocity potential $\phi(x,z)$ satisfies the Helmholtz equation

$$\left(\frac{\partial^2}{\partial x^2}+\frac{\partial^2}{\partial z^2}-k_y^2\right)\phi=0, \tag{1}$$

in the fluid domain.

Linearized free surface boundary condition at $z = 0$ is

$$\frac{\partial\phi}{\partial z}-\frac{\omega^2}{g}\phi=0, \tag{2}$$

where g is the acceleration of gravity. As fluid does not penetrate through seabed, prisms, and vertical wall, the boundary conditions are as follows

$$\frac{\partial\phi}{\partial z}=0,\ \text{at } z=-H,\ d<x<\infty \text{ and } z=-h,\ -L<x<d \tag{3a}$$

$$\frac{\partial \phi}{\partial x} = 0, \text{ at } x = d, \ -H < x < -h \ , \tag{3b}$$

$$\frac{\partial \phi}{\partial x} = 0, \text{ at } x = \pm d, \ h_{2j} < z < h_{2j-1}, \tag{4a}$$

$$\frac{\partial \phi}{\partial z} = 0, \text{ at z} = h_{2j-1}, h_{2j} \ \ -d < x < d, \text{ and} \tag{4b}$$

$$\frac{\partial \phi}{\partial x} = 0, \quad \text{at } x = -L, \ -h < z < \eta \ , \tag{5}$$

where j = 1 and 2 indicate prisms B1 and B2, respectively.

Along with the above boundary conditions, the velocity potential $\phi(x,z)$ satisfies the far-field radiation condition

$$\phi(x,z) \approx \left\{ Ie^{-ik_{0x}(x-d)} + Re^{ik_{0x}(x-d)} \right\} \frac{\cosh k_0(H+z)}{\cosh k_0 H}, \text{ as } x \to \infty, \tag{6}$$

where I and R are associated with the incident and reflected wave heights, respectively, in region R_1 and $k_{0x} = k_0 \cos \theta$ is the x-component of incident wave number k_0.

Using eigenfunction expansion method the velocity potentials $\phi_l(x,z)$ for each region R_l (where l = 1, 2, 3, 4 and 5) are computed. The velocity potentials $\phi_l(x,z)$ satisfy Eq. (1) along with the boundary conditions as in Eqs. (2) - (6). Proceeding in a similar manner as in Mondal and Takagi (2019), $\phi_l(x,z)$ are expressed as

$$\phi_1 = Ie^{-ik_{0x}(x-d)} + \sum_{n=0}^{\infty} A_n e^{ik_{nx}(x-d)} f_n(z), \tag{7}$$

$$\phi_2 = \sum_{n=0}^{\infty} \left(B_n \frac{\cos \mu_{nx} x}{\cos \mu_{nx} d} + C_n \frac{\sin \mu_{nx} x}{\sin \mu_{nx} d} \right) \psi_n(z), \tag{8}$$

$$\phi_3 = \sum_{n=0}^{\infty} \left(D_n \frac{\cosh p_{nx} x}{\cosh p_{nx} d} + E_n \frac{\sinh p_{nx} x}{\sinh p_{nx} d} \right) \varphi_n(z), \tag{9}$$

$$\phi_4 = \sum_{n=0}^{\infty} \left(F_n \frac{\cosh q_{nx} x}{\cosh q_{nx} d} + G_n \frac{\sinh q_{nx} x}{\sinh q_{nx} d} \right) \chi_n(z), \text{ and} \tag{10}$$

$$\phi_5 = \sum_{n=1}^{\infty} H_n \frac{\cos \kappa_{nx}(L+x)}{\cos \kappa_{nx}(L-d)} g_n(z), \tag{11}$$

where $f_n(z),\ \psi_n(z),\ \varphi_n(z),\ \chi_n(z)$ and $g_n(z)$ are eigenfunctions such that

$$f_n(z) = \frac{\cosh k_n(H+z)}{\cosh k_n H},\ \text{for } n = 0, 1, 2, ...,\ \text{and} \tag{12}$$

$$\varphi_n(z) = \begin{cases} 1,\ \text{for } n = 0 \\ \cos p_n(h_3 + z),\ \text{for } n = 1, 2, ... \end{cases} \tag{13}$$

The eigenfunctions $\psi_n(z)$ and $g_n(z)$ can be obtained from Eq. (12) replacing (k_n, H) by (μ_n, h_1) and (κ_n, h), respectively. In addition, the eigenfunction $\chi_n(z)$ can be obtained from Eq. (13) by replacing p_n and h_3 by q_n and h, respectively. The quantities, k_{nx}, μ_{nx}, p_{nx}, q_{nx} and κ_{nx}, which appear in Eqs. (7) - (11) are of the form

$$k_{nx} = \sqrt{k_n^2 - k_y^2},\ p_{nx} = \sqrt{p_n^2 + k_y^2},\ q_{nx} = \sqrt{q_n^2 + k_y^2},\ \mu_{nx} = \sqrt{\mu_n^2 - k_y^2},\ \kappa_{nx} = \sqrt{\kappa_n^2 - k_y^2}, \tag{14}$$

with $p_n = n\pi/(h_3 - h_2),\ q_n = n\pi/(h - h_4),$ and the wavenumber $\lambda_n \equiv (k_n, \mu_n, \kappa_n)$ satisfy the dispersion relation

$$\omega^2 = g\lambda_n \tanh \lambda_n \gamma\ , \tag{15}$$

where $\gamma = (H, h_1, h)$ and n = 0, 1, 2, ….

In Eqs. (7) – (11), A_n, B_n, C_n, D_n, E_n, F_n, G_n and H_n are unknown constants to be determined to know the velocity potentials completely. For the purpose of numerical computation, we need to truncate the infinite series over n. Suppose, the infinite series over A_n, B_n, C_n, D_n, E_n, F_n, G_n and H_n converge for n = N_1, N_2, N_3, N_4, N_5, N_6, N_7 and N_8. Therefore, we need to find out $\sum_{j=1}^{8}(N_j + 1)$ unknowns. For the purpose of simplicity, we consider N = max {N_1, N_2, …,N_8}. This gives (8N+8) unknowns which can be computed by considering matching conditions of velocity and pressure at $x = \pm d$.

4. NUMERICAL RESULTS AND DISCUSSION

In this section, hydrodynamic forces acting on the submerged prisms are computed for different physical parameters. The horizontal force (F_{x1}, F_{x2}) and vertical force (F_{z1}, F_{z2}), where subscripts 1 and 2 represent the prisms B1 and B2, respectively, are computed by

$$F_{xj} = i\rho\omega \int_{-h_{2j}}^{-h_{2j-1}} \left\{\phi_1(d,z) - \phi_5(-d,z)\right\} dz,\ j = 1, 2\ \text{ and} \tag{16}$$

$$F_{zj} = i\rho\omega \int_{-d}^{d} \left\{ \phi_{j+1}\left(x, h_{2j-1}\right) - \phi_{j+2}\left(x, h_{2j}\right) \right\} dx, \;\; j = 1, 2. \tag{17}$$

The hydrodynamic forces in non-dimensional form are

$$F_{xj}^{*} = \frac{F_{xj}}{\rho g H \zeta_a}, \;\; F_{zj}^{*} = \frac{F_{zj}}{\rho g H \zeta_a}, \tag{18}$$

where ζ_a is the incident wave amplitude.

For the purpose of numerical computation, the values of different parameters are h/H = 0.75, d/H = 0.25, s/H = 0.1, L/H = 1.0, and the incident wave angle θ = 30^{o}, unless otherwise stated. Before computing the numerical results, it is required to find the minimum value of N for which results converge. In the present context, we observed that the hydrodynamics forces converge for N = 20. Mondal and Takagi (2019) also found that the results converge for N = 20, in case of wave scattering by a single submerged prism.

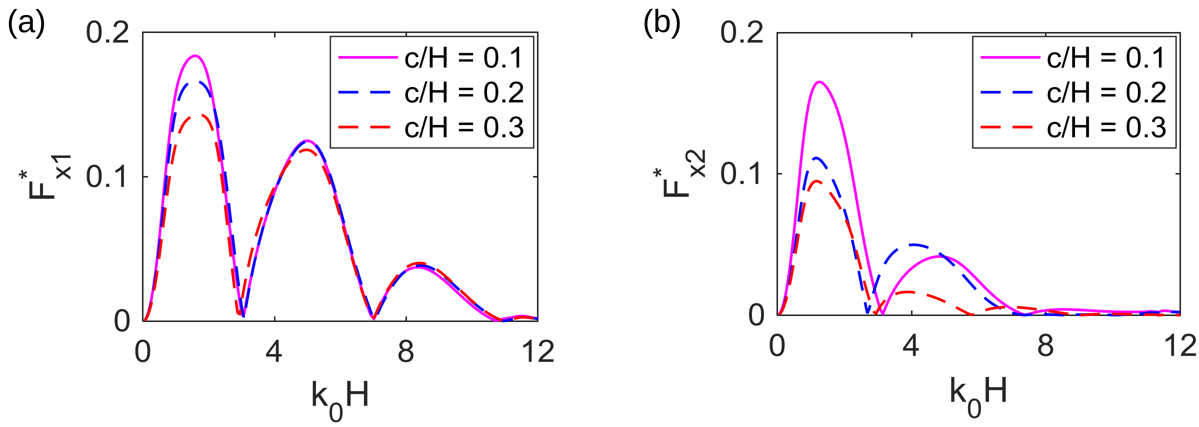

Fig. 2 Horizontal forces on prisms (a) B1 and (b) B2 for different values of c/H with h_1/H = 0.2.

Figs. 2 and 3 show the horizontal and vertical forces acting on the prisms for gap spacing c/H = 0.1, 0.2 and 0.3 when the upper prism B1 is placed at a fixed depth h_1/H = 0.2 from the mean free surface. The horizontal and vertical forces acting on the prism B1 tends to zero for non-dimensional wave number k_0H > 12 and 15, respectively. However, the forces on the prism B2 tends to zero at $k_0H \approx 8$. Both Figs. 2 and 3 depict that the hydrodynamic forces vary in a wavy fashion with increasing k_0H, the hydrodynamic forces becoming zero for different values of k_0H. The zero values result from the interaction between the incident wave and reflected wave from the vertical wall. The upper prism experiences more hydrodynamic force than the lower prism. With the increase in c/H, the maximum value of the horizontal force of the upper prism shrinks for k_0H < 1.7. As does that of the lower prism. The effect of c/H on the horizontal force of the upper prism is less than that the lower prism. This is because with increasing c/H

the lower prism gets closer to the seabed. The relationship between the vertical force and *c/H* is not straight forward as that between the horizontal force and *c/H* (Fig. 2). With increasing *c/H*, the vertical force on the upper prism decreases for k_0H = 0.01 - 1.82 but enhances for k_0H = 1.82 – 5.34. For the lower prism, *c/H* = 0.1 produces the largest force for k_0H = 0.01 – 3.5.

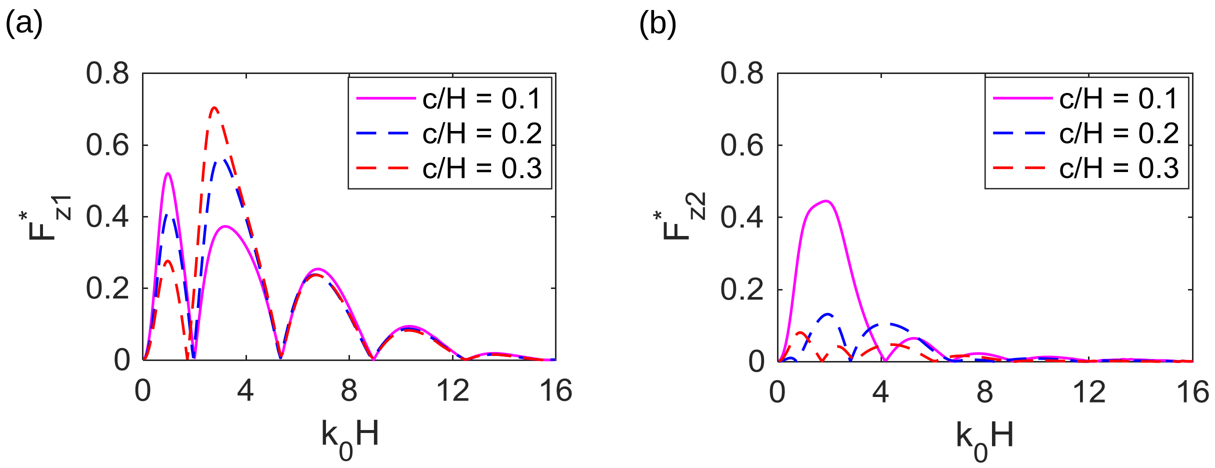

Fig. 3 Vertical forces on prisms (a) B1 and (b) B2 for different values of *c/H* with h_1/H = 0.2.

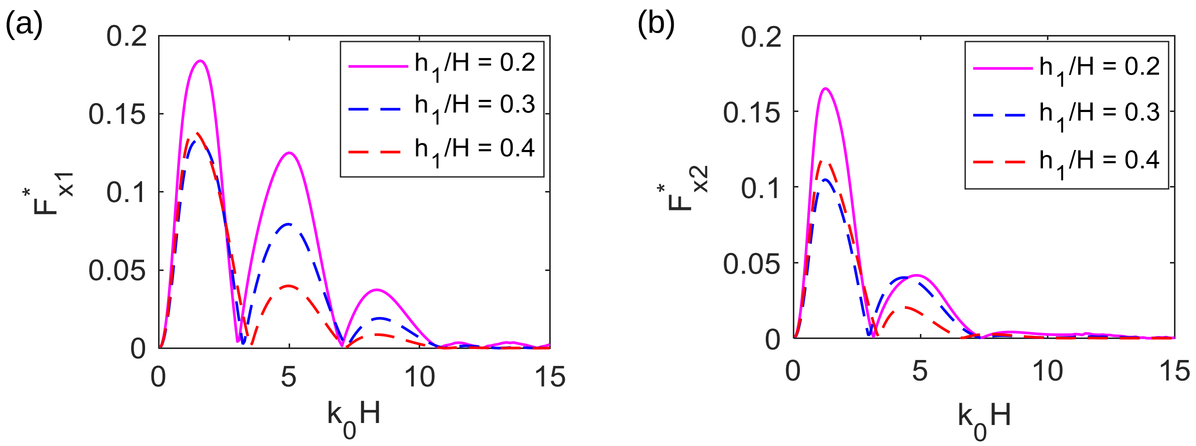

Fig. 4 Horizontal forces on the prisms (a) B1 and (b) B2 for different values of h_1/H with *c/H* = 0.1.

Figs. 4 and 5 show the variation in horizontal and vertical forces with k_0H for h_1/H = 0.1, 0.2 and 0.3 when *c/H* = 0.1. It is observed that horizontal force on B1 increase with k_0H for k_0H = 0.1 – 1.6. Reaching a maximum at k_0H = 1.6, it declines with further increasing k_0H and become zero. However, the horizontal force on lower prism reaches a maximum at a lower value of k_0H = 0.97 and with the increase of k_0H, declines in magnitude attending a zero minimum. This process continues, leading to a damped wavy variation of the forces with k_0H. The amplitude of the forces decreases with increasing k_0H. Furthermore, it is observed that the forces decrease with the increase in c/H and h_1/H.

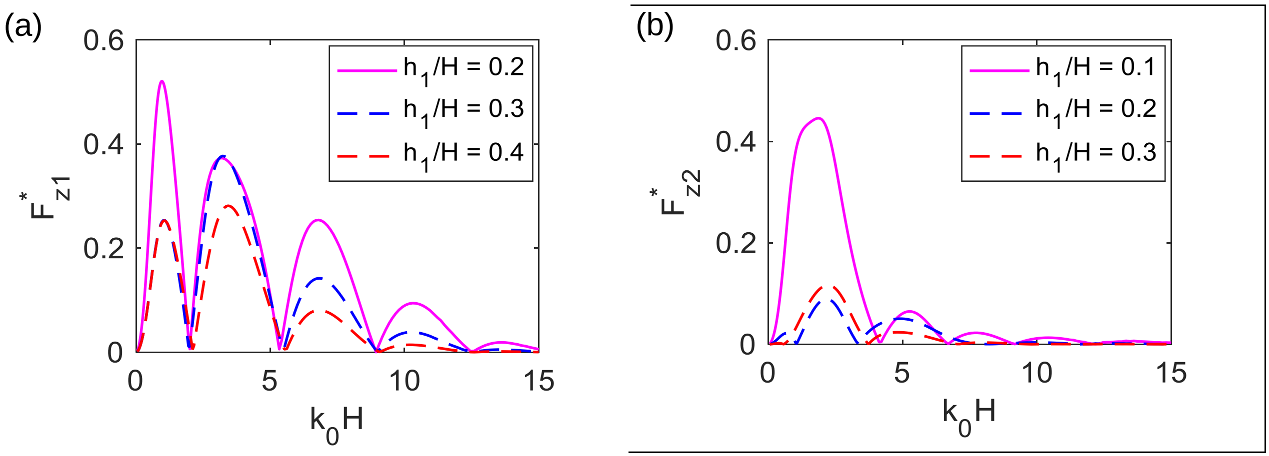

Fig. 5 Vertical forces on the prisms (a) B1 and (b) B2 for different values of h_1/H with c/H = 0.1.

3. CONCLUSIONS

In the present study, we formulated a boundary value problem for oblique water wave scattering by two fixed submerged prisms in the presence of a vertical step and the fluid domain is considered semi-infinite in nature. The problem is solved analytically by using the Fourier expansion method. The velocity potentials are described explicitly in terms of infinite series solution. It is observed that for the present set of numerical values of different physical parameters, hydrodynamics forces converge for the truncated values N = 20. Therefore, this technique is more convenient than any other numerical methods (e.g. finite element method, boundary integral method) in terms of cost and computation time. It is found that the horizontal and vertical forces vary in a wavy pattern with k_0H and the amplitude of forces decreases with the increase of k_0H. The horizontal and vertical forces acting on the upper prism are negligible for $k_0H > 12$. However, the lower prism experience negligible force at smaller $k_0H \approx 8$. With the decrease of submergence depth (h_1/H), the maximum value of horizontal force increases. The gap spacing (c/H) has a negligible effect on horizontal force acting on the upper prism (Fig. 1). However, it is observed that the wave force acting on the lower prism decrease significantly with the increase of c/H. This happens as the lower prism's depth increase with the increase of c/H. The findings are likely to be useful for the modeling of submerged breakwaters.

REFERENCES

Cheong, H.F., Shankar, N.J. and Nallayarasu, S. (1996), "Analysis of submerged platform breakwater by eigenfunction expansion method," *Ocean Eng.*, **23**(8), 649-666.

Hu, H. Wang, K.H. and Williams, A.N. (2002), "Wave motion over a breakwater system of a horizontal plate and a vertical porous wall," *Ocean Eng.*, **29**, 373-386.

Liu, P.L.F. and Iskandarani, M. (1991), "Scattering of short-wave groups by submerged horizontal plate," *J. Waterway., Port, Coastal and Ocean Eng.*, **117**(3), 235-246.

Liu, Y., Li, Y. and Teng, B. (2009), "Wave motion over two submerged layers of horizontal thick plates," *J. Hydrodynamics*, **21**(4), 453-462.

Mondal, R. and Takagi, K. (2019), "Wave scattering by a fixed submerged platform over a step bottom," *Proc IMechE Part M: J Eng Maritime Env.,* **233**, 93-107.

Patarapanich, M. and Cheong, H.F. (1989), "Reflection and transmission characteristics of regular and random waves from from a submerged horizontal plates," *Coastal Eng.*, **13**, 161-182.

Patarapanich, M. (1984), "Maximum and zero reflection from submerged plate," *J. Waterway., Port, Coastal and Ocean Eng.*, **110**(3), 171-181.

Wang, K.H. and Shen, Q. (1999), "Wave motion over a group of submerged horizontal plates," *Int. J . Eng. Science*, **37**, 703-715.

Zheng, Y.H., Shen, Y.M. and Tang, J. (2007), "Radiation and diffraction of linear water waves by an infinitely long submerged rectangular structure parallel to a vertical wall," *Ocean Eng.*, **34**, 69-82.

Zheng, Y.H., Liu, P.F., Shen, Y.M., Wu, B.J. and Sheng, S.W. (2007), "On the radiation and diffraction of linera water waves by an infinitely long rectangular structure submerged in oblique sea," *Ocean Eng*., **34**, 436-450.